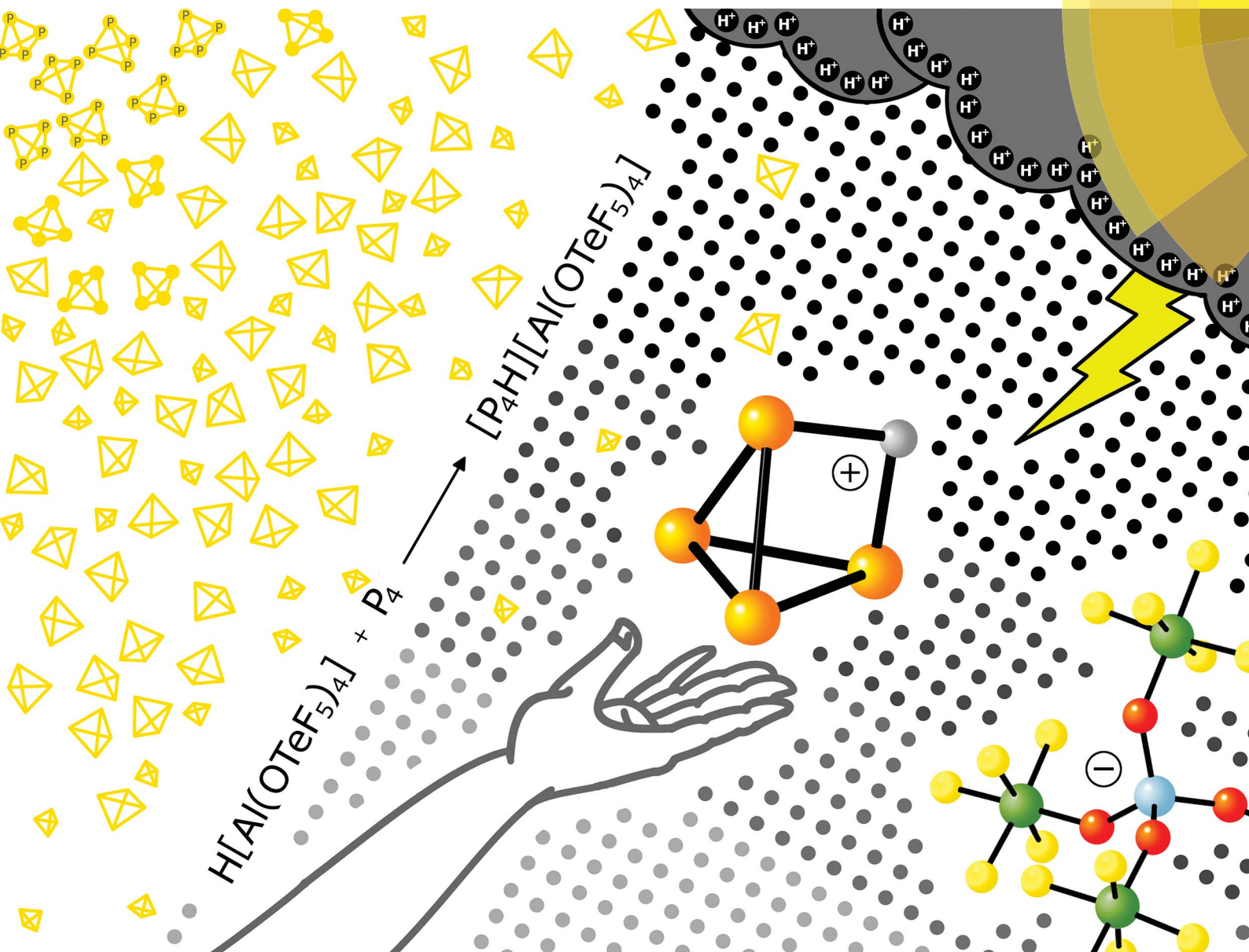


# Chemical Science

rsc.li/chemical-science



ISSN 2041-6539



## EDGE ARTICLE

Christian Müller, Sebastian Riedel *et al.*

$[\text{P}_4\text{H}]^+[\text{Al(OTeF}_5)_4]^-$ : protonation of white phosphorus with the Brønsted superacid  $\text{H[Al(OTeF}_5)_4]_{\text{soln}}$

Cite this: *Chem. Sci.*, 2018, 9, 7169

All publication charges for this article have been paid for by the Royal Society of Chemistry

# $[P_4H]^+[Al(OTeF_5)_4]^-$ : protonation of white phosphorus with the Brønsted superacid $H[Al(OTeF_5)_4]_{(solv)}^{\dagger\dagger}$

Anja Wiesner,<sup>†</sup> Simon Steinhauer,<sup>†</sup> Helmut Beckers, Christian Müller<sup>†\*</sup> and Sebastian Riedel<sup>†\*</sup>

A sustainable transformation of white phosphorus ( $P_4$ ) into chemicals of higher value is one of the key aspects in modern phosphorus research. Even though the chemistry of  $P_4$  has been investigated for many decades, its chemical reactivity towards the simplest electrophile, the proton, is still virtually unknown. Based on quantum-chemical predictions, we report for the first time the successful protonation of  $P_4$  by the Brønsted acid  $H[Al(OTeF_5)_4]_{(solv)}$ . Our spectroscopic results are in agreement with acid-mediated activation of  $P_4$  under protonation of an edge of the  $P_4$ -tetrahedron and formation of a three-center two-electron P–H–P bond. These investigations are of fundamental interest as they permit the activation of  $P_4$  with the simplest electrophile as a new prototype reaction for this molecule.

Received 8th July 2018  
Accepted 10th August 2018

DOI: 10.1039/c8sc03023e

rsc.li/chemical-science

## Introduction

White phosphorus ( $P_4$ ), discovered by Henning Brand in 1669 while searching for the philosopher's stone, is the thermodynamically least stable and most reactive form of phosphorus at room temperature and consists of tetrahedral  $P_4$  molecules. Despite its spontaneous flammability and severe toxicity,  $P_4$  is the easiest form to produce on an industrial scale and is therefore the commercially most important allotrope.<sup>1</sup> Especially its conversion to  $PCl_3$  is of high interest, as it is a base chemical for the production of many organophosphorus compounds.

From a historical point of view, two important chemical reactions of  $P_4$  are described in every good textbook of inorganic chemistry:<sup>2</sup> (a) the slow oxidation of  $P_4$  vapor to  $P_4O_{10}$  under emission of light. This chemoluminescence has coined the name phosphorus, which is derived from the greek mythology ("light-bearer"). (b) the activation and disproportionation of  $P_4$  by aqueous solutions of alkali metal hydroxides. In this way, the industrially relevant phosphine gas ( $PH_3$ ) is obtained in high purity next to the alkali metal salt of hypophosphorous acid ( $NaH_2PO_2$ ). More recent studies deal with the degradation of white phosphorus in the presence of other strong nucleophiles, such as organolithium and organomagnesium compounds, carbenes or silylenes, under the topic " $P_4$ -activation and functionalization".<sup>3–6</sup> From a mechanistic point of view, a charged

nucleophile ( $Nu^-$ ) interacts with one of the three energetically degenerate LUMOs of the  $P_4$  molecule (Fig. 1a) under opening of the  $P_4$  tetrahedron to yield a substituted butterfly-like bicyclo [1,1,0]tetraphospha-butane anion (Fig. 1b, I).<sup>7</sup>

Electrophiles, on the other hand, should react at an edge of the tetrahedron, as the two energetically degenerate highest occupied molecular orbitals (HOMO and HOMO–1) have large coefficients at two adjacent phosphorus atoms (Fig. 1a). The situation is, however, much more complicated and the formation of various products is usually observed in this seemingly simple reaction. In the case of  $Ph_2P^+$  and  $NO^+$ , the insertion of these small molecules into one of the P–P bonds is indeed observed, as also theoretically predicted for  $NO^+$  (Fig. 1b, II).<sup>9–11</sup> In the case of  $Ag^+$  as an example of an electrophilic transition metal center, a weak coordination of  $Ag^+$  to the edge of the  $P_4$  tetrahedron occurs (Fig. 1b, III).<sup>12</sup> However, depending on the steric demand of the metal fragment, the coordination of  $P_4$  via the apex can be enforced, even though the interaction of the energetically low-lying HOMO–5 with the electrophile is necessary to achieve this coordination mode (Fig. 1b, IV).<sup>13</sup>

In contrast to the experimental observations made for the reaction of  $P_4$  with nucleophiles as well as coordinatively and electronically unsaturated transition metal complexes, experimental proof for the structure of the elusive  $[P_4H]^+$  cation in solution is still missing in the literature. In fact, weak acids do not react with  $P_4$  due to the rather poor nucleophilicity and weak basicity of white phosphorus. Common strong acids, such as sulfuric acid ( $H_2SO_4$ ) and nitric acid ( $HNO_3$ ) cannot be used for the generation of  $[P_4H]^+$  as they directly oxidize  $P_4$  to either phosphorous acid ( $H_3PO_3$ ) and sulfur dioxide ( $SO_2$ ), or to phosphoric acid ( $H_3PO_4$ ), nitrogen oxide ( $NO_2$ ) and water ( $H_2O$ ), respectively. Hydrogen chloride (HCl) can react with  $P_4$  to form

Institut für Chemie und Biochemie, Freie Universität Berlin, Fabeckstr. 34/36, 14195 Berlin, Germany. E-mail: c.mueller@fu-berlin.de; s.riedel@fu-berlin.de

<sup>†</sup> Dedicated to Prof. Dr Peter Jutzi on the occasion of his 80<sup>th</sup> birthday.

<sup>‡</sup> Electronic supplementary information (ESI) available. See DOI: 10.1039/c8sc03023e

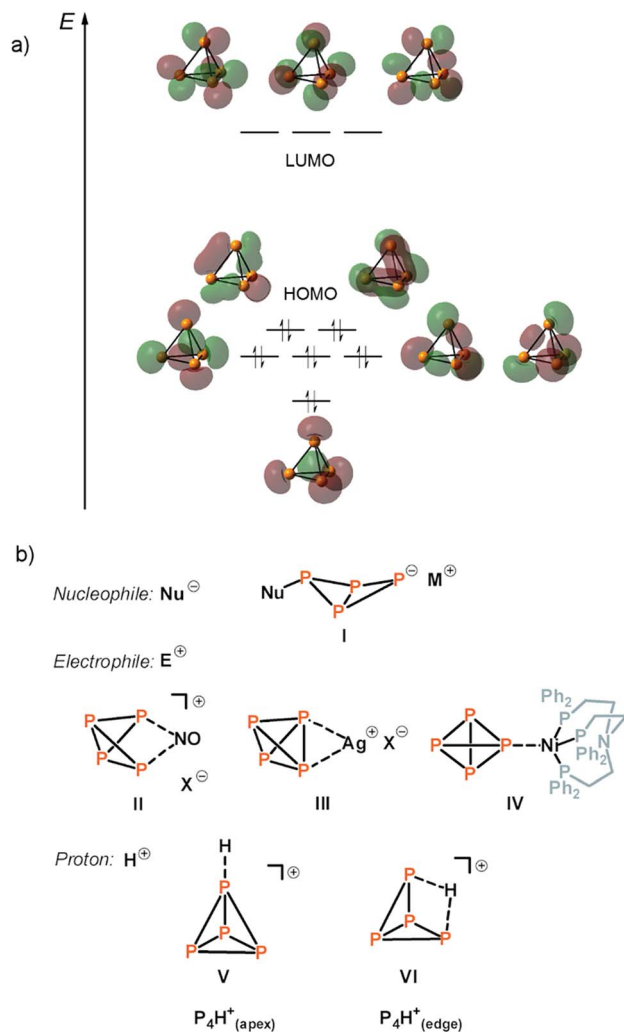


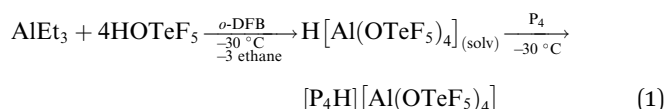
Fig. 1 Molecular orbital scheme of P<sub>4</sub> (a)<sup>8</sup> and examples of nucleophilic and electrophilic attacks at P<sub>4</sub> and the assumed structures for protonated P<sub>4</sub> (b).

phosphine gas (PH<sub>3</sub>) and phosphorus trichloride (PCl<sub>3</sub>). Based on *ab initio* calculations, Fluck *et al.*<sup>14</sup> predicted in 1979 that the weakly bound proton in [P<sub>4</sub>H]<sup>+</sup> is located at the apex of the tetrahedron (Fig. 1b, V), while protonation at the edge was predicted to be energetically less favored (Fig. 1b, VI). The authors exclude protonation at the P<sub>3</sub>-face. More recent *ab initio* molecular orbital calculations at the MP2/6-31G(d,p) level of theory in 1996 by Abboud, Yáñez and co-workers reveal, however, that the thermodynamically most favourable process is the protonation at the edge under formation of a three-center two-electron (3c-2e) P–H–P bond (Fig. 1b, VI).<sup>15</sup> The same group determined the gas-phase basicity of P<sub>4</sub> by means of Fourier transform ion cyclotron resonance mass spectrometry. In 2000, Ponc and co-workers provided an additional theoretical support for the existence of a non-classical 3c-2e P–H–P bond in [P<sub>4</sub>H]<sup>+</sup> using the generalized population analysis.<sup>16</sup> More recently, Lobayan and Bochicchio used a topological analysis of the electron density to describe the 3c-2e P–H–P bond in [P<sub>4</sub>H]<sup>+</sup>.<sup>17</sup>

## Results

Taking the above-mentioned considerations into account, we anticipated that strong acids of conjugated weakly coordinating and non-reactive anions should be excellent reagents for the protonation of P<sub>4</sub>. Reed and Nixon, for instance, have shown that phosphabenzene can be protonated by the *in situ* generated Brønsted superacid H(CHB<sub>11</sub>Me<sub>5</sub>Br<sub>6</sub>).<sup>18</sup> Also these phosphorus heterocycles are known for their extremely weak basicity. As one of us<sup>19</sup> has recently reported a novel aluminum-based superacidic system containing the weakly coordinating anion [Al(OTeF<sub>5</sub>)<sub>4</sub>]<sup>−</sup>, we report here now the synthesis and the first spectroscopic proof on the structure of [P<sub>4</sub>H]<sup>+</sup> in solution.

According to quantum-chemical calculations at the B3LYP/def2-TZVPP level, the protonation of P<sub>4</sub> can be achieved by a medium consisting of the Brønsted superacid H[Al(OTeF<sub>5</sub>)<sub>4</sub>]<sub>(solv)</sub> and *ortho*-difluorobenzene (*o*-DFB), see eqn (1).<sup>19</sup> This is due to a slightly lower proton affinity of *o*-DFB (741.6 kJ mol<sup>−1</sup>) compared to P<sub>4</sub> (748.4 kJ mol<sup>−1</sup>), as computed at CCSD(T)/aug-cc-pVTZ level of theory.



The reaction product of P<sub>4</sub> and the Brønsted superacid was obtained as a temperature-, moisture- and oxygen-sensitive salt. It shows a clean low-temperature proton-coupled <sup>31</sup>P NMR spectrum with two equally intense signals at δ = −481.7 and δ = −405.8 ppm with a weak roof effect (Fig. 2a). No other signals were observed in the <sup>31</sup>P NMR spectrum in the region between δ = 400 ppm and δ = −800 ppm.

This spectrum, which also reveals an additional splitting owing to the higher order of the system, is in accordance with an AX<sub>2</sub>Y<sub>2</sub> spin system (<sup>1</sup>J(<sup>31</sup>P<sub>X</sub>, <sup>31</sup>P<sub>Y</sub>) = 233.95 Hz, <sup>1</sup>J(<sup>1</sup>H<sub>A</sub>, <sup>31</sup>P<sub>Y</sub>) = 36.70 Hz, <sup>2</sup>J(<sup>31</sup>P<sub>X</sub>, <sup>1</sup>H<sub>A</sub>) = 4.91 Hz). This can only result from the protonation of the P<sub>4</sub> molecule at the P–P-edge. Furthermore, a triplet of triplets at δ = −5.35 ppm appears in the <sup>1</sup>H NMR spectrum (Fig. 2c) showing the corresponding couplings of the proton to P<sub>X</sub> and P<sub>Y</sub>, respectively. Interestingly, both the chemical shifts and coupling constants are in excellent agreement with the simulated spectra of [P<sub>4</sub>H]<sub>(edge)</sub><sup>+</sup>, obtained by quantum-chemical calculations (Fig. 2b and c and S3, Table S1†). For comparison reasons, Fig. 2d shows the simulated <sup>31</sup>P NMR spectrum of the species [P<sub>4</sub>H]<sub>(apex)</sub><sup>+</sup>, which clearly differs from the experimental results. The NMR studies clearly prove the presence of [P<sub>4</sub>H][Al(OTeF<sub>5</sub>)<sub>4</sub>] and that P<sub>4</sub> is protonated at an edge of the tetrahedron as predicted by quantum-chemical calculations.<sup>15–17</sup>

We further started to investigate the dynamics of the cation in solution. Interestingly, variable temperature NMR spectroscopy indicates a coalescence of the signals at T = −10 °C (Fig. 3).

The triplet of triplets observed at T = −40 °C in the <sup>1</sup>H NMR spectrum broadens with increasing temperature resulting in a broad singlet (approx. FWHM = 75 Hz) at the coalescence temperature. The chemical shift slightly changes from δ =





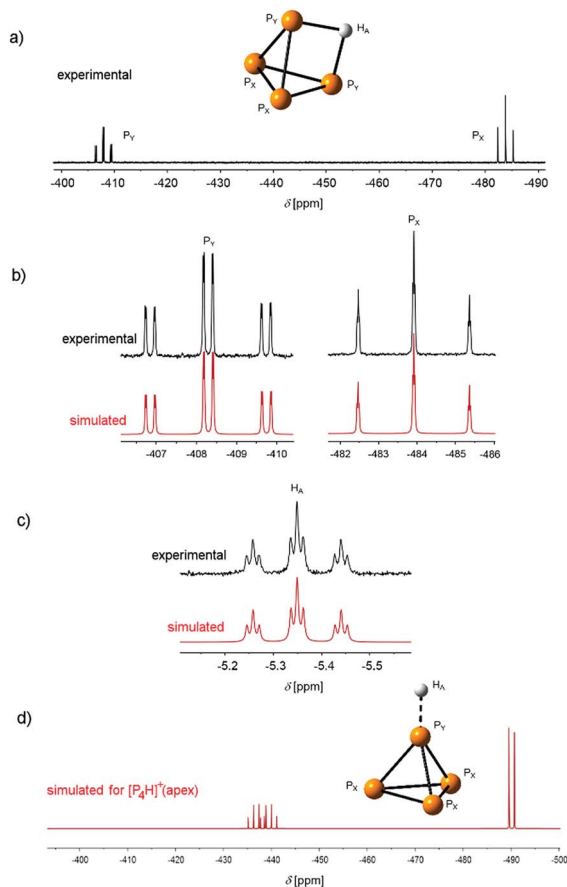


Fig. 2 (a) Low-temperature ( $T = -40\text{ }^{\circ}\text{C}$ ) experimental  $^{31}\text{P}$  NMR spectra of  $[\text{P}_4\text{H}][\text{Al}(\text{OTeF}_5)_4]$  in *o*-DFB (external lock:  $[\text{D}_6]\text{acetone}$ ). The atom labelling is indicated in accordance with the  $\text{AX}_2\text{Y}_2$  spin system. (b)  $^{31}\text{P}$  NMR spectrum (162 MHz, top) and simulated  $\text{P}_\text{X}$  and  $\text{P}_\text{Y}$  signals (bottom) of the species  $[\text{P}_4\text{H}]_{(\text{edge})}^+$ . (c) Experimental and simulated  $^1\text{H}$  NMR spectrum (401 MHz). The full spectra are provided in Fig. S1 and S2.† (d) Simulated  $^{31}\text{P}$  NMR  $\text{P}_\text{X}$  and  $\text{P}_\text{Y}$  signals of the species  $[\text{P}_4\text{H}]_{(\text{apex})}^+$ .

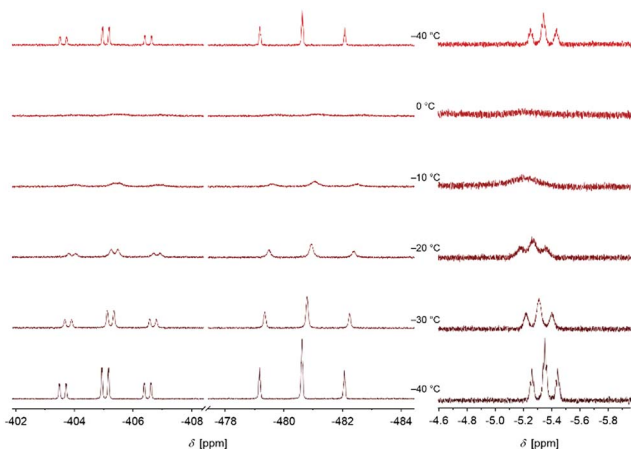


Fig. 3 Excerpt of the  $^{31}\text{P}$  and  $^1\text{H}$  NMR spectra of  $[\text{P}_4\text{H}][\text{Al}(\text{OTeF}_5)_4]$  in *o*-DFB (external lock:  $[\text{D}_6]\text{acetone}$ ) at various temperatures. The sample was first measured at  $T = -40\text{ }^{\circ}\text{C}$ , annealed stepwise to  $T = 0\text{ }^{\circ}\text{C}$  and cooled down again to  $T = -40\text{ }^{\circ}\text{C}$  afterwards.

$-5.35\text{ ppm}$  at  $T = -40\text{ }^{\circ}\text{C}$  to  $\delta = -5.19\text{ ppm}$  at  $T = 0\text{ }^{\circ}\text{C}$ . In the  $^{31}\text{P}$  NMR spectrum, a similar process is observed. The two signals are broadened at the coalescence temperature and shifted to a higher field by  $0.5\text{ ppm}$  for  $\text{P}_\text{X}$  and  $\text{P}_\text{Y}$  at  $T = 0\text{ }^{\circ}\text{C}$ . This process is reversible by re-cooling the sample to  $T = -40\text{ }^{\circ}\text{C}$  again. No signal for  $\text{P}_4$  is detected during this process. Based on these observations, we anticipate a dynamic intramolecular migration of the proton on the  $\text{P}_4$  surface. From the experimental dynamic-NMR data, the corresponding barrier can be estimated to  $\Delta G^\ddagger = 54.2\text{ kJ mol}^{-1}$ .

We noticed, that if an excess of  $\text{P}_4$  is present in the reaction mixture, the previously described  $[\text{P}_9]^+$  cation<sup>20</sup> is formed next to  $[\text{P}_4\text{H}]^+$ . Upon warming a sample containing a mixture of  $[\text{P}_4\text{H}]^+$  and  $\text{P}_4$  from  $T = -40\text{ }^{\circ}\text{C}$  to  $T = -10\text{ }^{\circ}\text{C}$ , a fast and full conversion to  $[\text{P}_9]^+$  is observed, as detected by NMR spectroscopy. This observation indicates that activation of the  $\text{P}_4$  molecule by protonation already occurs at low temperature, while broad band UV/Vis irradiation is necessary to form  $[\text{P}_9]^+$  from a  $\text{P}_4/[\text{P}_4\text{NO}]^+$  mixture, as reported in the literature before.<sup>10</sup>

The  $[\text{P}_4\text{H}]^+$  cation was further analyzed by means of mass spectrometry. In the mass spectrum (positive mode), a signal allocated to  $[\text{P}_4\text{H}]^+$  appears at  $m/z = 124.9$ . In addition, signals due to  $[\text{P}_4]^+$  ( $m/z = 123.8$ ) as well as of  $[\text{Te}]^+$  and  $[\text{TeH}]^+$  in a natural isotope distribution ( $n = 122, 124\text{--}126$ ) arise with less intensity. Furthermore, the cations  $[\text{P}_3]^+$ ,  $[\text{o-DFB}]^+$ ,  $[\text{o-DFB-H}]^+$  and  $[\text{P}_5]^+$  were found. The mass spectrum recorded in the negative mode shows only signals of the four anions  $[\text{AlF}_3(\text{OTeF}_5)]^-$ ,  $[\text{AlF}_2(\text{OTeF}_5)_2]^-$ ,  $[\text{AlF}(\text{OTeF}_5)_3]^-$  and  $[\text{Al}(\text{OTeF}_5)_4]^-$ , see Fig. S7–S9.†

Finally, we investigated  $[\text{P}_4\text{H}][\text{Al}(\text{OTeF}_5)_4]$  by means of Raman spectroscopy both in an *o*-DFB solution at  $T = -30\text{ }^{\circ}\text{C}$  and as a neat powder at  $T = -78\text{ }^{\circ}\text{C}$  in the solid state (Fig. 4). In both spectra, two prominent bands can be observed. The band around  $\tilde{\nu} = 1615\text{ cm}^{-1}$  corresponds to the symmetrical P–H–P stretching mode and the band at  $\tilde{\nu} = 598\text{ cm}^{-1}$  occurs slightly

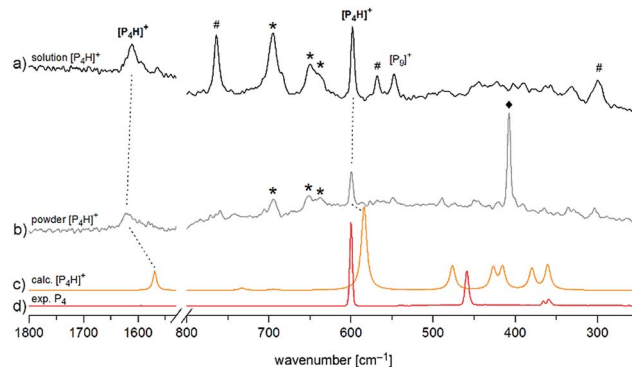


Fig. 4 Enlarged Raman spectrum of (a)  $[\text{P}_4\text{H}][\text{Al}(\text{OTeF}_5)_4]$  in *o*-DFB at  $T = -30\text{ }^{\circ}\text{C}$  and (b)  $[\text{P}_4\text{H}][\text{Al}(\text{OTeF}_5)_4]$  washed with *n*-pentane at  $T = -78\text{ }^{\circ}\text{C}$ , (c) calculated spectrum of  $[\text{P}_4\text{H}]^+$  at the B3LYP/def2-TZVPP level of theory and (d) experimental spectrum of solid  $\text{P}_4$  at  $T = -196\text{ }^{\circ}\text{C}$ . Bands of the anion  $[\text{Al}(\text{OTeF}_5)_4]^-$  at  $\tilde{\nu} = 695, 650$  and  $637\text{ cm}^{-1}$  are marked by an asterisk (\*). Bands of the solvent (*o*-DFB: #, *n*-pentane: ♦) are indicated as well. Full spectra are provided in Fig. S5 and S6.†



shifted with respect to the breathing mode of neat  $P_4$  and is assigned to the corresponding mode of  $[P_4H]^+$ .

Both the experimental band positions agree well with the computed wavenumbers at the B3LYP/def2-TZVPP level of theory at  $\tilde{\nu} = 1569\text{ cm}^{-1}$  ( $A_1$ ) and  $\tilde{\nu} = 584\text{ cm}^{-1}$  ( $A_1$ ), respectively. Further Raman bands are predicted between  $\tilde{\nu} = 360\text{ cm}^{-1}$  and  $\tilde{\nu} = 476\text{ cm}^{-1}$  but they are difficult to assign in the experimental spectrum due to their rather low intensities and their partial interference with the bands of  $[P_9]^+$  impurities. It should be pointed out that special care must be taken by isolating  $[P_4H][Al(OTeF_5)_4]$  as a solid, as one sample exploded during the Raman measurement at dry ice temperature after approx. 300 scans at 75 mW, Fig. 4b. Attempts to record low-temperature IR spectra of the  $[P_4H]^+$  cation were unsuccessful, as the strongest IR band of  $[P_4H]^+$  is hidden by very prominent bands of the anion at  $\tilde{\nu} = 713\text{ cm}^{-1}$  and  $\tilde{\nu} = 695\text{ cm}^{-1}$ . Also, the strongest band of  $o$ -DFB occurs at  $\tilde{\nu} = 750\text{ cm}^{-1}$ . Nevertheless, low temperature ( $T = -30\text{ }^\circ\text{C}$ ) IR spectra of the liquid phase of  $[P_4H][Al(OTeF_5)_4]$  have been recorded using a glass fiber ATR head, which are provided in Fig. S10 and S11.†

Our quantum-chemical calculations at the coupled-cluster CCSD(T)/aug-cc-pVTZ level agree very well with the experimental results of the protonation of a  $P_4$  edge. This position is also expected from the MO diagram, where the HOMO orbital is located along the  $P_4$  edge (Fig. 1a), leading to a three-center two-electron P–H–P bond. This gives rise to a  $C_{2v}$  symmetric structure with an elongation of the  $P_Y \cdots P_Y$  bond of 20.4 pm compared to the bond length of 221.8 pm in the  $P_4$  tetrahedral structure. The bond distances  $P_Y-P_X$  and  $P_X-P_X$  are less affected by 1.4 and 6.3 pm, respectively (Fig. 5). The computed minimum structure for protonation at the apex of the  $P_4$  molecule is 61.4  $\text{kJ mol}^{-1}$  higher in energy than the global minimum structure. An apex protonation would also lead to a computed P–H stretching mode at  $\tilde{\nu} = 2502\text{ cm}^{-1}$ , which is more than  $\tilde{\nu} = 900\text{ cm}^{-1}$  above the experimentally observed band at  $\tilde{\nu} = 620\text{ cm}^{-1}$ . Surprisingly, the protonation and simultaneous opening of the tetrahedral structure lead to a  $P_4$ -butterfly type minimum structure (Fig. 5), while protonation of the triangle surface shows a higher order saddle point. Both structures will be higher in energy by 74.3 and 88.5  $\text{kJ mol}^{-1}$  compared to the

global minimum structure of  $[P_4H]^+$ , see Fig. 5. For details of the computed structural parameters see Tables S2 and S3.†

## Conclusions

Based on these results, we could reveal for the first time the structure of protonated white phosphorus in solution. Both experimental results and quantum-chemical calculations provide evidence for a protonation at the edge of the  $P_4$  molecule. The opening of the  $P_4$ -tetrahedron *via* the simplest electrophile ( $H^+$ ) under formation of a three-center two-electron P–H–P bond is of fundamental interest for understanding the reactivity of this intriguing phosphorus allotrope. It is expected that this groundbreaking result is important for the development of chemical processes related to the activation and further functionalization of elemental phosphorus by electrophiles.

## Conflicts of interest

There are no conflicts to declare.

## Acknowledgements

This work was supported by the Freie Universität Berlin and Deutsche Forschungsgemeinschaft (GRK 1582, Fluorine as a Key Element). We thank Dr Andreas Springer from the Core Facility BioSupraMol at the FU Berlin for measuring the mass spectra. Computing time was made available by High-Performance Computing at ZEDAT/Freie Universität Berlin.

## Notes and references

- 1 F. Krafft, *Angew. Chem., Int. Ed. Engl.*, 1969, **8**, 660.
- 2 R. Steudel, *Chemie der Nichtmetalle, Synthesen - Strukturen - Bindung - Verwendung de Gruyter*, Berlin, edn 4, 2014.
- 3 M. Scheer, G. Balázs and A. Seitz, *Chem. Rev.*, 2010, **110**, 4236.
- 4 (a) J. E. Borger, A. W. Ehlers, M. Lutz, J. Chris Slootweg and K. Lammertsma, *Angew. Chem., Int. Ed.*, 2014, **53**, 12836; (b) L. Xu, Y. Chi, S. Du, W.-X. Zhang and Z. Xi, *Angew. Chem., Int. Ed.*, 2016, **55**, 9187; (c) M. Arrowsmith, M. S. Hill, A. L. Johnson, G. Kociok-Köhn and M. F. Mahon, *Angew. Chem., Int. Ed.*, 2015, **54**, 7882.
- 5 (a) J. D. Masuda, W. W. Schoeller, B. Donnadiou and G. Bertrand, *Angew. Chem., Int. Ed.*, 2007, **46**, 7052; (b) J. D. Masuda, W. W. Schoeller, B. Donnadiou and G. Bertrand, *J. Am. Chem. Soc.*, 2007, **129**, 14180; (c) O. Back, G. Kuchenbeiser, B. Donnadiou and G. Bertrand, *Angew. Chem., Int. Ed.*, 2009, **48**, 5530; (d) D. Martin, M. Soleilhavoup and G. Bertrand, *Chem. Sci.*, 2011, **2**, 389; (e) C. L. Dorsey, B. M. Squires and T. W. Hudnell, *Angew. Chem., Int. Ed.*, 2013, **52**, 4462; (f) C. D. Martin, C. M. Weinstein, C. E. Moore, A. L. Rheingold and G. Bertrand, *Chem. Commun.*, 2013, **49**, 4486; (g) M. Cicač-Hudi, J. Bendi, S. H. Schlindwein, M. Bispinghoff, M. Nieger, H. Grützmaier and D. Gudat, *Eur. J. Inorg. Chem.*, 2016, **5**, 649.

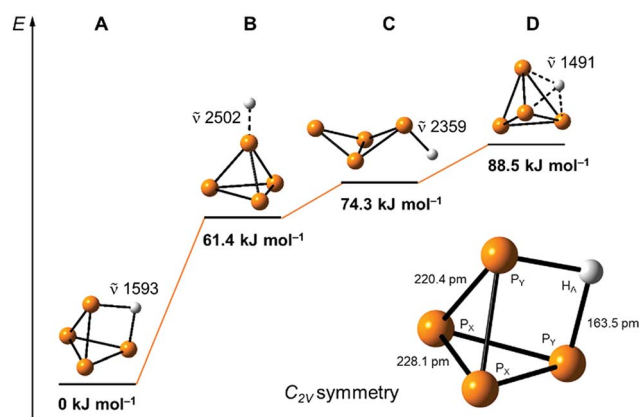


Fig. 5 Computed relative energies and P–H vibrations of optimized  $[P_4H]^+$  structures at the CCSD(T)/aug-cc-pVTZ level of theory.



- 6 (a) Y. Xiong, S. Yao, M. Brym and M. Driess, *Angew. Chem.*, 2007, **119**, 4595; (b) S. Khan, R. Michel, S. S. Sen, H. W. Roesky and D. Stalke, *Angew. Chem., Int. Ed.*, 2011, **50**, 11786.
- 7 R. Riedel, R. H.-D. Hausen and E. Fluck, *Angew. Chem.*, 1985, **97**, 1050.
- 8 B. M. Cossairt and C. C. Cummins, *J. Am. Chem. Soc.*, 2009, **131**, 15501.
- 9 J. J. Weigand, M. Holthausen and R. Fröhlich, *Angew. Chem.*, 2009, **121**, 301.
- 10 T. Köchner, S. Riedel, A. J. Lehner, H. Scherer, I. Raabe, T. A. Engesser, F. W. Scholz, U. Gellrich, P. Eiden, R. A. Paz Schmidt, D. A. Plattner and I. Krossing, *Angew. Chem., Int. Ed.*, 2010, **49**, 8139.
- 11 K. F. Hoffmann, A. Wiesner, N. Subat, S. Steinhauer, S. Riedel and Z. Anorg, *Z. Anorg. Allg. Chem.*, 2018, DOI: 10.1002/zaac.201800174.
- 12 I. Krossing and L. van Wüllen, *Chem. - Eur. J.*, 2002, **8**, 700.
- 13 (a) P. Dapporto, S. Midollini and L. Sacconi, *Angew. Chem., Int. Ed.*, 1979, **18**, 469; (b) M. Peruzzini, S. Mañas, A. Romerosa and A. Vacca, *Mendeleev Commun.*, 2000, **10**, 134; (c) T. Gröer, G. Baum and M. Scheer, *Organometallics*, 1998, **17**, 5916.
- 14 E. Fluck, C. M. E. Pavlidou and R. Janoschek, *Phosphorus Sulfur Relat. Elem.*, 1979, **6**, 469.
- 15 J.-L. M. Abboud, M. Herreros, R. Notario, M. Esseffar, O. Mó and M. Yáñez, *J. Am. Chem. Soc.*, 1996, **118**, 1126.
- 16 R. Bochicchio, L. Lain, A. Torre and R. Ponc, *Croat. Chem. Acta*, 2000, **73**, 1039.
- 17 R. M. Lobayan and R. Bochicchio, *J. Phys. Chem. A*, 2015, **119**, 7000.
- 18 Y. Zhang, F. S. Tham, J. F. Nixon, C. Taylor, J. C. Green and C. A. Reed, *Angew. Chem., Int. Ed.*, 2008, **47**, 3801.
- 19 A. Wiesner, T. W. Gries, S. Steinhauer, H. Beckers and S. Riedel, *Angew. Chem., Int. Ed.*, 2017, **56**, 8263.
- 20 T. Köchner, T. A. Engesser, H. Scherer, D. A. Plattner, A. Steffani and I. Krossing, *Angew. Chem., Int. Ed.*, 2012, **51**, 6529.

